Molecular Biology of the Cell
Vol. 15, 3005–3014, July 2004

The *Drosophila* tctex-1 Light Chain Is Dispensable for Essential Cytoplasmic Dynein Functions but Is Required during Spermatid Differentiation[D]

Min-gang Li,* Madeline Serr,* Eric A. Newman,† and Thomas S. Hays*‡

*Departments of Genetics, Cell, and Developmental Biology, and †Neuroscience, University of Minnesota, St. Paul, Minnesota 55108

Submitted January 8, 2004; Revised April 7, 2004; Accepted April 8, 2004
Monitoring Editor: David Drubin

Variations in subunit composition and modification have been proposed to regulate the multiple functions of cytoplasmic dynein. Here, we examine the role of the *Drosophila* ortholog of tctex-1, the 14-kDa dynein light chain. We show that the 14-kDa light chain is a bona fide component of *Drosophila* cytoplasmic dynein and use P element excision to generate flies that completely lack this dynein subunit. Remarkably, the null mutant is viable and the only observed defect is complete male sterility. During spermatid differentiation, the 14-kDa light chain is required for the localization of a nuclear "cap" of cytoplasmic dynein and for proper attachment between the sperm nucleus and flagellar basal body. Our results provide evidence that the function of the 14-kDa light chain in *Drosophila* is distinct from other dynein subunits and is not required for any essential functions in early development or in the adult organism.

INTRODUCTION

The minus-end–directed microtubule motor cytoplasmic dynein has been implicated in a variety of cellular processes, including nuclear envelope breakdown, mitotic spindle assembly and orientation, chromosome movements, intracellular trafficking of organelles and mRNAs, and intraflagellar transport (reviewed in Karki and Holzbaur, 1999). The heavy chain subunit of dynein is known to provide ATPase and microtubule binding functions, and although more than one cytoplasmic dynein heavy chain has been identified, the major cytoplasmic dynein motor contains a homodimer of a single heavy chain. It remains unclear how this single cytoplasmic dynein motor is targeted to distinct organelles and cellular processes. One hypothesis is that the accessory intermediate, light intermediate, and light chain subunits of cytoplasmic dynein mediate its functional specialization. Consistent with this idea, in some eukaryotes these subunits are encoded by multiple genes that are differentially expressed and/or alternatively spliced as distinct transcripts in different tissues and cells (Gill *et al*., 1994; Pfister *et al*., 1996a; Bowman *et al*., 1999; Susalka *et al*., 2000; Tynan *et al*., 2000; Tai *et al*., 2001). In addition, the posttranslational modification of subunits may contribute to the heterogeneity of subunit composition in the dynein complex (Pfister *et al*., 1996b). Although the mutational analysis of the cytoplasmic dynein heavy chain has revealed a range of motor functions, the functional contribution of other individual subunits is not well understood.

The present study addresses the function of the 14-kDa dynein light chain. This light chain was first identified as a cytoplasmic dynein subunit in mammalian brain (King *et al*., 1996a) and as an axonemal dynein subunit within the specialized inner arm dynein of the *Chlamydomonas* flagella (Harrison *et al*., 1998). In *Drosophila*, a molecular study of the 14-kDa light chain gene reported defective male fertility for hypomorphic alleles, but the nature of the mutations left unresolved the significance of the 14-kDa light chain in cytoplasmic dynein (Caggese *et al*., 2001). Sequence analysis revealed that the 14-kDa dynein light chain is the product of a previously cloned mouse gene, *tctex-1* (Lader *et al*., 1989; King *et al*., 1996b). The *tctex-1* gene is part of the mouse *t*-complex, a chromosomal region that has been implicated in "transmission ratio distortion," also referred to as "meiotic drive" (reviewed in Silver 1993; Olds-Clarke, 1997). One hypothesis is that distorted segregation results from mutations in dynein genes within the *t*-complex that contribute to the misregulation of axonemal assembly and motility (King *et al*., 1996b; Harrison *et al*., 1998).

Significantly, the physical interaction of tctex-1 homologs with a variety of proteins in mammalian cells, including Doc2 (Nagano *et al*., 1998), CD5 (Bauch *et al*., 1998), Fyn kinase (Kai *et al*., 1997; Campbell *et al*., 1998), Trk kinase (Yano *et al*., 2001) rhodopsin (Tai *et al*., 2001), and poliovirus receptor CD155 (Mueller *et al*., 2002), suggests that tctex light chain also serves multiple cytoplasmic functions. However, the in vivo functional analysis of tctex-1 in vertebrates is made more difficult by multiple genes that encode related polypeptides. In mouse, there are four known copies of the *tctex-1* gene on chromosome 17 and in humans, a second gene, *rp3*, encodes a relatively divergent 14-kDa protein (55% identity) that can compete with the tctex-1 isoform for incorporation into the dynein complex (Tai *et al*., 2001).

In *Drosophila*, the ortholog of the *tctex-1* gene was first reported as the dynein light chain 90F (*Dlc90F*; Li *et al*., 1998). *Drosophila* tctex (dtctex) protein is encoded by a single gene (Li *et al*., 1998; Caggese *et al*., 2001; this study), but its role in cytoplasmic dynein function is not well characterized. To test whether this light chain might direct a specific

Article published online ahead of print. Mol. Biol. Cell 10.1091/mbc.E04–01–0013. Article and publication date are available at www.molbiolcell.org/cgi/doi/10.1091/mbc.E04–01–0013.

[D] Online version of this article contains supporting material. Online version is available at www.molbiolcell.org.

‡ Corresponding author. E-mail address: tom-h@biosci.cbs.umn.edu.

cytoplasmic dynein function in *Drosophila*, we have generated a null mutation in the gene and characterized the null phenotype. Our results demonstrate that although this light chain is a bona fide component of dynein motors in multiple tissues, it is absolutely required only in spermatogenesis and is therefore the first dynein subunit found to be nonessential in *Drosophila*.

MATERIALS AND METHODS

Fly Stocks

The fly stocks of P element insertion lines *l(3)05822/TM3*, *ry Sb Ser*, and *l(3)05089/TM3*, and deficiency *Df(3R)DG2/TM2* (89E1-F4; 91B1-2) were obtained from the Bloomington Drosophila Stock Center (Bloomington, IN). The *ru h st* p^p *ss* e^s stock was obtained from the Bowling Green Stock Center (Bowling Green State University, Bowling Green, OH)) and was isogenized in this laboratory for a lethal-free third chromosome. The Δ2-3 source of transposase was provided by a stock *Df(3)/TM3 Sb* Δ2-3 obtained from our colleague Dr. Michael Simmons (University of Minnesota, St. Paul, MN). The p50-green fluorescent protein (GFP) transgenic line was described previously (Wojcik *et al*., 2001). Oregon R flies were used as wild-type controls. Flies were raised on standard yeast-cornmeal-agar medium at 25°C.

Polymerase Chain Reaction (PCR) Reactions

The coding region of the *Dlc90F* gene was obtained by amplification of cDNAs derived from a 2- to 14-h embryonic library, by using sense primer 5′-GATGGATGACTCACGCGAAG-3′ (base pairs 161–180) and the antisense primer 5′-GGCAGTCCTGCCATTCCTCC-3′ (base pairs 500–520 of the cDNA sequence; GenBank no. 708968). PCR products were subcloned into the pGEM-T vector (Promega, Madison, WI). In screening for deletions of *Dlc90F*, template DNA was isolated from single male flies according to the method of Engels *et al.* (1990) with minor modifications. A single fly was homogenized with a pipette tip in 50 μl of buffer containing 10 mM Tris-Cl, pH 8.2, 1 mM EDTA, 25 mM NaCl, and 200 μg/ml proteinase K. After incubation at 37°C for 20 min, the solution was heated at 95°C for 2 min. Two microliters of DNA were used as a template, with sense primer 5′-GAA TGA ACG TGG CTT GCA G-3′ located 390 bp upstream of the cDNA, and antisense primer 5′-CAA TTG CTG CCA TGG AAA CG-3′, which is 310 base pairs 3′ to the polyadenylation site of the *Dlc90F* transcript. A predicted PCR fragment from wild-type genomic DNA is 1249 bp. In the excision experiment, we screened for a PCR fragment either bigger or smaller than the wild type.

DNA and RNA Hybridization

Genomic DNA for Southern blot experiments was prepared from adult flies as described previously (Rasmusson *et al*., 1994). Southern and Northern blots were prepared by standard methods. Hybridizations were carried out in a solution of 40% formamide, 5% dextran sulfate, 5 × SSCP, pH 6.8, 50 mM Tris-HCl, pH 7.5, 1× Denhardt's solution, 1% SDS, and 0.1 mg/ml single-strand salmon sperm DNA at 42°C for overnight. Final washes were 2× SSC, 0.2% SDS at 42°C for low-stringency and 0.1× SSC, 0.1% SDS at 65°C for high-stringency conditions. The cosmid genomic DNA clone was isolated by screening a cosmid library made from *iso-1* fly DNA (Tamkun *et al*., 1992), by using the *Dlc90F* coding region as a probe.

Antibodies and Protein Analysis

A polyclonal antiserum "1246" was raised in rabbits against the synthesized peptide "DDSREESQFIVDDVSC," and affinity purified over a column of the same peptide bound to agarose gel (procedures carried out by QCB). Extracts from whole flies and fly tissues were made in PMEG buffer (100 mM PIPES, pH 6.9, 5 mM MgOAc, 5 mM EGTA, 0.1 mM EDTA, 0.5 mM dithiothreitol, and 0.9 M glycerol) plus protease inhibitors (10 μg/ml aprotinin, 1 μg/ml leupeptin and pepstatin, 0.1 μg/ml each of soybean trypsin inhibitor, *n*-tosyl-L-arginine methyl ester, and benzamidine). Preparation of crude dynein by ATP-sensitive affinity to taxol-stabilized microtubules was as described previously (Hays *et al*., 1994). Sedimentation of crude dynein or soluble extracts of tissues through 5–20% sucrose gradients was as described previously (McGrail *et al*., 1995). Immunoprecipitation experimental procedures were as described previously (Boylan *et al*., 2000). SDS-PAGE used 5–17% acrylamide gradient gels. Western blots were probed with anti-light chain (LC) 1246 diluted 1:3000; anti-dynein heavy chain (HC) monoclonal antibody P1H4 (McGrail and Hays, 1997) diluted 1:10,000; anti-dynein intermediate chain (Chemicon International, Temecula, CA) diluted 1:1500 and processed with the Tropix chemiluminescent system (Applied Biosystems, Foster City, CA).

Meiotic Recombination and P Excision

Lethal mutations on the chromosomes *l(3)05822* and *l(3)05089* were removed by meiotic recombination of the chromosomes with a lethal-free third chromosome containing multiple genetic markers, *ru h st* p^p *ss* e^s. The lethal-free P insertion chromosome derived from *l(3)05089* was renamed *F5*. For P excision experiments, flies of genotype *F5*, *ry/TM6B D* were mass mated to *Df(3)/TM3 Sb*, Δ2-3. Individual *F5/TM3 Sb*, Δ2-3 males were then crossed to *l(3)/TM3 Sb*, *ry* females. From each vial, one progeny male with rosy eyes (Δ*P/TM3 Sb*, *ry*) was selected and crossed to *l(3)/TM3 Sb*, *ry* females. Three days later, DNA templates for PCR were prepared from single male flies, and the resulting products were screened for altered migration of DNA fragments on gels. Once a candidate was identified, the balanced progeny of Δ*P*, *ry/TM3 Sb*, *ry* from the crosses with the male were used to establish a stock.

Cytology

Testes were dissected from 1- to 2-d-old males in TB1 (15 mM potassium phosphate, pH 6.7, 80 mM KCl, 16 mM NaCl, 5 mM $MgCl_2$, and 1% polyethylene glycol 8000) and placed on Superfrost Plus slides (Fisher Scientific. Pittsburgh, PA). Testes on slides were either ruptured to expose spermatogenic cysts or left intact. Coverslips were added onto the samples, and the slides were immediately frozen in liquid nitrogen. The coverslips were removed with a razor blade, and the slides were placed in methanol on dry ice for 15 min., washed with phosphate-buffered saline (PBS), and then PBS + 0.1% Triton X-100 (PBT) and blocked with PBT/bovine serum albumin (BSA) (PBT + 1% BSA) at room temperature for 45 min. Slides were incubated with antibodies in PBT/BSA at room temperature for 2 h or at 4°C for overnight in a humid chamber. After washing in PBT and PBS, slides were incubated with secondary antibodies for 1 h at room temperature in a darkened humid chamber. Slides were washed in PBS and mounted in PBS/90% glycerol with 1 mg/ml *p*-phenylenediamine. Images were collected on a Yokogawa spinning disk confocal with Ultraview software (PerkinElmer Life and Analytical Sciences, Boston, MA) and processed in Adobe Photoshop.

DNA was visualized with Oligreen (Molecular Probes, Eugene, OR) diluted 1:200. F-actin was visualized with rhodamine-conjugated phalloidin (Sigma-Aldrich, St. Louis, MO) (200 μg/μl). Anti-dynein HC monoclonal P1H4 was diluted 1:250. Anti-cnn rabbit polyclonal antibody (gift of T. Kaufman) was diluted 1:500. Anti-γ-tubulin monoclonal GTU88 (Sigma-Aldrich) was diluted 1:250. Secondary antibodies conjugated to Alexa488 or Alexa568 (Molecular Probes) were diluted 1:200.

For cytological analysis of spermiogenesis, testes were dissected from newly eclosed males, fixed, and stained with both Oligreen, to visualize spermatid nuclei, and phalloidin to highlight individualization. In wild-type testes, all 64 nuclei were fully elongated and properly bundled at the distal tip of individual postmeiotic cysts. An average of 32 such cysts were seen in each testis (n = 16). In mutant testes, all cysts contained mislocalized nuclei that were distributed throughout the cyst and elongated spermatid tails. Some mutant cysts did contain a subset of fully elongated nuclei at the tip of the testis (average 6 cysts per testis, n = 22). However, the number of normally positioned nuclei at the tips of these cysts was always <64.

Electroretinogram Recordings and Examination of Rhabdomere Morphology

Morphology of rhabdomeres was examined using the optical neutralization technique described by Franceschini and Kirschfeld, 1971. Electroretinograms (ERGs) were recorded from nonanesthetized flies immobilized with polyethylene glycol monooleyl ether, a low melting point wax. Recordings were made DC (1-KHz low pass filtered) by using low-resistance micropipettes filled with saline solution. The active electrode was placed on the surface of the eye and the ground electrode on the thorax. Conductive electrode gel was used to improve the contact between the pipettes and the fly. White light stimuli were focused onto the eye through a 10× microscope objective and were gated by an electromagnetic shutter. Responses were recorded and analyzed using a Labview data acquisition interface and custom software.

A 4-s light flash evoked a potential with a sustained negative ON response, which decayed slowly with time, and a large transient OFF response (see supplemental Figure 1). We compared the amplitude of the ON response in *e155/e155* flies to *+/e155* sibling controls, which should not have a mutant phenotype. The ON response amplitude averaged 16.1 ± 1.1 mV (SD, n = 8) in *+/e155* flies and 16.0 ± 1.0 (9) mV in *e155/e155* flies. The two amplitudes are not significantly different (p = 0.41, unpaired *t*-test). The decay of both the ON and OFF responses occurred at similar rates for the two groups of flies.

RESULTS

The Tctex-1 Homolog Is a Component of Cytoplasmic Dynein in Drosophila

We initiated our study of the function of the 14-kDa dynein LC in *Drosophila* development by isolating a cosmid genomic DNA clone, by using a cDNA probe that encodes the fly homolog of the mouse *tctex-1* gene. A restriction map of the *Dlc90F* genomic region and the nearest flanking genes on either side are shown in Figure 1A. Our Southern blot anal-

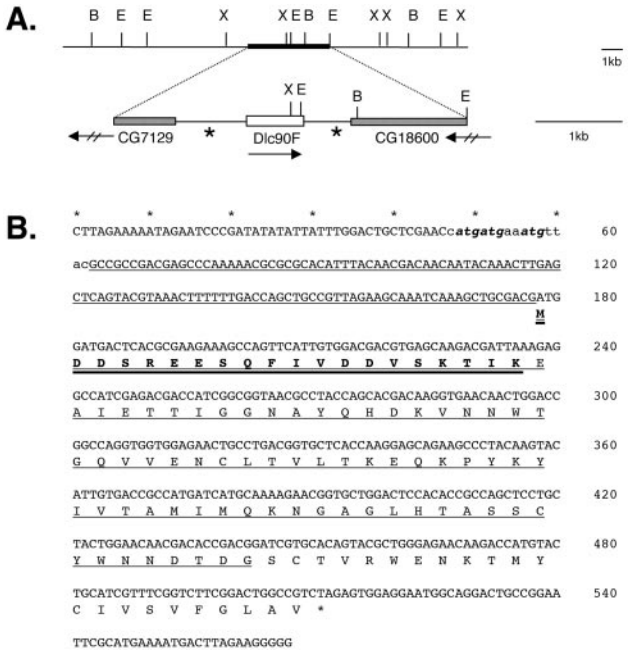

Figure 1. The *Dlc90F* gene. (A) Restriction enzyme map of the genomic region of a cloned cosmid. Enzyme abbreviations are B, *Bam*HI; E, *Eco*RI; and X, *Xba*I. Position and orientation of transcription are indicated for *Dlc90F* and two flanking genes, *CG7129* and *CG18600*. Expressed sequence tag clones representing both genes are identified in the *Drosophila* genome project: LD44138 for *CG7129* and LD14124 for *CG18600*. Asterisks indicate positions of PCR primers used in the PCR screen for deletion of *Dlc90F*. (B) Nucleotide and deduced amino acid sequences of *Dlc90F*. Underlined letters indicate sequences deleted in the *e155* chromosome. Lowercase letters are footprints left by excision of the P element. A peptide used to generate an antibody against the 14-kDa LC is double underlined. Three ATG codons preceding the internal in-frame ATG codon are highlighted with bold italicized letters.

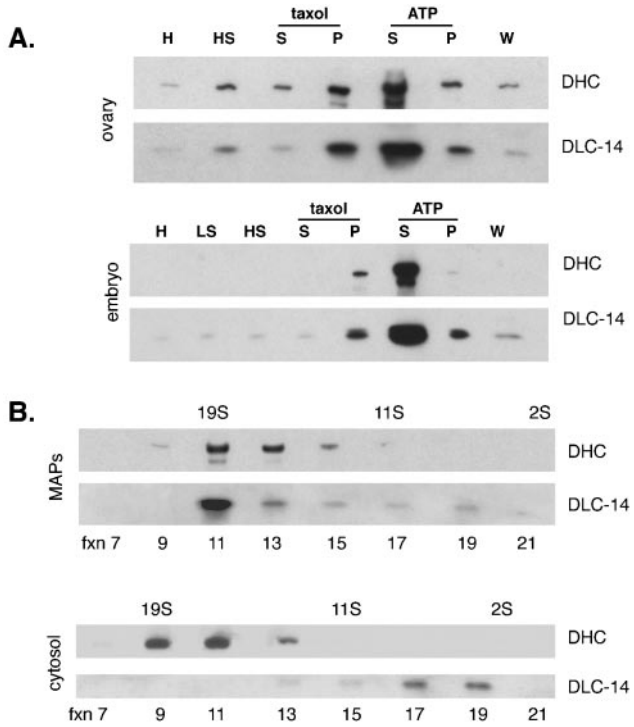

Figure 2. The 14-kDa LC protein is part of the dynein motor complex in ovaries and embryos. (A) Proteins were purified by affinity to microtubules. Endogenous tubulin in extracts from ovaries and embryos was stabilized by the addition of taxol and pelleted under conditions depleting ATP. The pellet was washed once, and then eluted with MgATP. Equal total protein from each fraction was separated by SDS-PAGE, blotted, and probed with antibodies against the 14-kDa LC and the dynein heavy chain. The 14-kDa LC shows a pattern of enrichment similar to the dynein heavy chain in both tissues. H, homogenate; LS, low-speed supernatant; HS, high-speed supernatant; W, wash; S, supernatant; P, pellet. (B) When the ATP-release fraction from A is further purified over density gradients, the 14-kDa LC remains in the dynein motor complex ~19S. In contrast, gradient purification of soluble extracts (not enriched for dynein) reveals much of the 14-kDa LC is not in the dynein complex, unlike the dynein heavy chain. Equal volumes of fractions from 5–20% sucrose gradients were analyzed by Western blotting. Positions of sedimentation standards run in parallel gradients are indicated above the panels.

yses of genomic DNA by using the *Dlc90F* coding region as a probe detect a single band under both high- and low-stringency conditions, indicating that a single copy of the *Dlc90F* gene is present in the genome of *Drosophila melanogaster*. This conclusion is consistent with the sequence data from the *Drosophila* genome project and with other reports (Caggese *et al*., 2001). Sequence comparisons of genomic DNA and cDNA reveal no introns in the *Dlc90F* gene. Northern blots of total RNA isolated from different developmental stages and tissues show that the gene transcribes an ~0.6-kb mRNA throughout development, with enrichment in ovaries and early embryos (our unpublished data; Caggese *et al*., 2001). This expression pattern is similar to that observed for the *Dhc64C* gene encoding the principle cytoplasmic dynein heavy chain in *D. melanogaster* (Li *et al*., 1994).

To examine whether the *Dlc90F* gene product is assembled into the cytoplasmic dynein motor complex in *Drosophila*, we generated a polyclonal antibody against a peptide derived from the first 20 residues of *Dlc90F* (Figure 1B). On Western blots, the antibody recognizes a band of mobility ~14 kDa in extracts isolated from whole flies and individual tissues. This polypeptide is enriched in dynein prepared by microtubule affinity from both ovaries and embryos (Figure 2A). After further purification of the ATP-eluted dynein fraction by sucrose density gradient sedimentation, the 14-kDa polypeptide cosediments with the ~19S dynein complex, indicating that this light chain is present as a subunit within the dynein complex (Figure 2B). Immunoprecipitation experiments by using antibodies against the cytoplasmic dynein HC, IC, and 14-kDa LC subunits confirm they exist as a complex in embryos and ovaries (our unpublished data).

In addition, we observe a pool of 14-kDa LC that is not complexed with dynein. When cytosolic extracts, rather than crude dynein preparations, are fractionated through sucrose gradients, the majority of the 14-kDa subunit sediments outside the complex, with a lower S value (Figure 2B).

The 14-kDa LC Is Required for Male Fertility

To analyze the function of the 14-kDa LC during *Drosophila* development, we carried out a mutational analysis of the *Dlc90F* gene. Using restriction fragment length polymorphism analysis, we confirmed that a deficiency in the region *Df(3R)DG2* contains a deletion removing the *Dlc90F* gene (supplemental Figure 2). A P element insertion line,

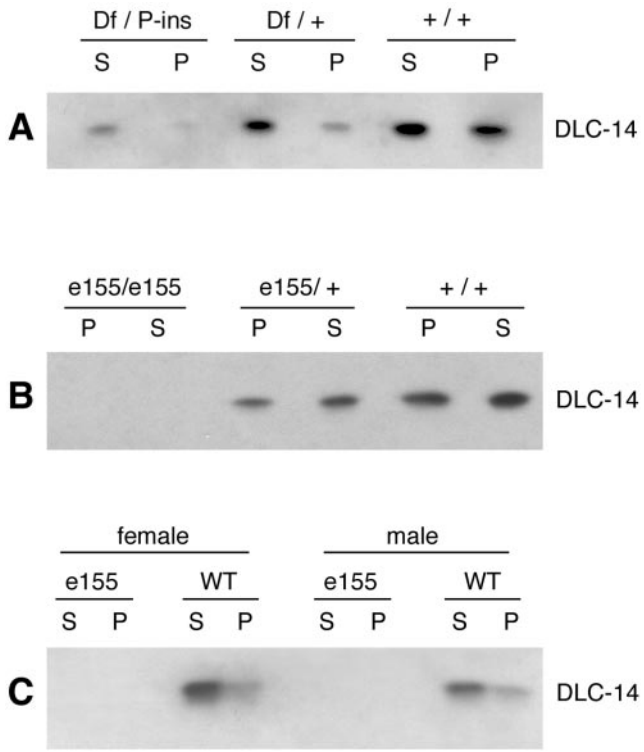

Figure 3. A P element insertion results in partial loss-of-function of *Dlc90F*, and imprecise excision of the P element abolishes 14-kDa LC expression. (A) A Western blot probed with the 14-kDa LC antibody. Ovary extracts were centrifuged to separate insoluble material, and equal total protein was loaded in each lane. LC expression in flies of genotype *Df(3R)DG2/F5* is reduced but not eliminated. (B) Ovary extracts were prepared as in A from the P excision line *e155/e155*, balanced siblings with one copy of *Dlc90F* (*e155/+*), and wild-type (+/+). (C) No protein is detected in extracts from whole male or female adult flies homozygous for *e155*. WT, wild-type; S, supernatant; P, pellet.

l(3)05089, was obtained and shown by Southern blot experiments to contain a single insertion. Plasmid rescue and sequence analysis indicated that the P element is located within the 5′ untranslated region (UTR) of the *Dlc90F* transcript. Although the P-insertion chromosome is homozygous lethal, complementation tests with the deficiency show that flies of genotype *l(3)05089/Df(3R)DG2* are viable, suggesting that the lethal mutation in the stock is not a result of the P insertion. We removed the background lethal mutation by meiotic recombination. Because the original name of the stock, *l(3)05089*, was based on the lethal phenotype, we redesignated the lethal-free P chromosome *F5*. Flies homozygous for *F5* or hemizygous for *F5/Df(3R)DG2* are viable and male flies are sterile.

To demonstrate that the observed male sterility is associated with the P insertion, the P element was excised from its position by using a P element transposase. Of 11 excisions examined, three lines were homozygous viable and fertile, indicating that the P insertion disrupts the function of the *Dlc90F* gene and that the 14-kDa LC is required for male fertility. Because the P element is inserted in the 5′ UTR of *Dlc90F* transcript, we tested whether the insertion abolished expression of *Dlc90F*. As shown in Figure 3A, by using the antibody specific for the 14-kDa LC in Western blot experiments, the amount of the 14-kDa LC protein is substantially reduced in the hemizygous mutant (*Df/F 5*) flies compared with the heterozygous siblings or wild-type flies; however, some protein of the expected size is still produced. This result demonstrates that the P element insertion leads to a partial loss-of-function of *Dlc90F*.

Previously, we have shown that cytoplasmic dynein function is essential for cell viability and *Drosophila* development (Gepner *et al*., 1996). To determine whether the function of the 14-kDa LC is also essential, we isolated a null mutation of *Dlc90F* by imprecise excision of the P element from the *F5* chromosome. Analysis of the *Drosophila* genome reveals that the *Dlc90F* gene is closely flanked by genes on either side (Figure 1A; BDGP database). Expressed sequence tag clones representing both genes are identified in the *Drosophila* genome project, indicating they are bona fide genes. To generate a mutation that removes only the *Dlc90F* gene, we first conducted P element excision screens by selecting loss of an eye marker carried by the P element and then identified by PCR a deletion that removes the *Dlc90F* gene. Of 75 excision events scored, one, designated *e155*, produced a PCR fragment shorter than wild type (see supplemental Figure 2). Sequence analysis demonstrated that the chromosome in *e155* contains a 381-bp deletion in the *Dlc90F* gene. The 5′ break point is at the position where the P element is originally inserted (bp 46 in the 5′ UTR of the cDNA) and the 3′ break point is at bp 426 of the cDNA. This deletion removes the translation initiation codon and most of the coding sequence of *Dlc90F* (Figure 1B). The P element excision also leaves a 16-bp footprint in the insertion site. Thus, the predicted transcript of the deleted *Dlc90F* gene in *e155* flies is 200 nt and, if translated from an internal in-frame methionine codon, would produce a peptide of 12 residues derived from the C terminus of the 14-kDa LC. However, due to the insertion of the 16-bp P element footprint, three out-of-frame ATG codons have been created, which are likely to prevent the use of the internal methionine codon of *Dlc90F*. Furthermore, structural analysis of the 14-kDa LC has predicted that the last 12 aa correspond to a β-sheet that has no predicted function (Mok *et al*., 2001; Makokha *et al*., 2002). Consistent with these molecular data, the epitope recognized by the 14-kDa LC antibody is not detected in *e155* homozygotes (Figure 3). We conclude that *e155* represents a null mutation of *Dlc90F*.

Flies homozygous for *e155/e155* and hemizygous for *e155/Df(3R)DG2* are viable and males are sterile. When homozygous *e155/e155* females are mated with heterozygous *e155/+* males, equal numbers of homozygous and heterozygous progeny are produced, suggesting that neither maternal nor zygotic expression of the 14-kDa LC is needed for normal development in flies. We found no distorted segregation of *tctex-1* in the mutant. Both mutant and wild-type sperm are able to fertilize eggs, and no abnormal ratio of genotypes in the progeny is observed. Our data demonstrate that although the 14-kDa light chain is a bona fide component of *Drosophila* cytoplasmic dynein, its function in the cytoplasmic motor is not essential and is dispensable for most developmental processes in *Drosophila*.

No Effect on Rhabdomere Formation and Function

It has been shown that the mammalian tctex-1 dynein light chain can directly bind the cytoplasmic tail of the transmembrane protein rhodopsin (Tai *et al*., 1998). Rhodopsin is a visual light transduction protein; mutations affecting rhodopsin and its localization can promote degeneration of photoreceptors and cause retinitis pigmentosa. The polarized transport of rhodopsin-containing vesicles in vertebrate cell extracts was reported to depend on cytoplasmic dynein (Tai *et al*., 1999). In *Drosophila*, the analogous trafficking of

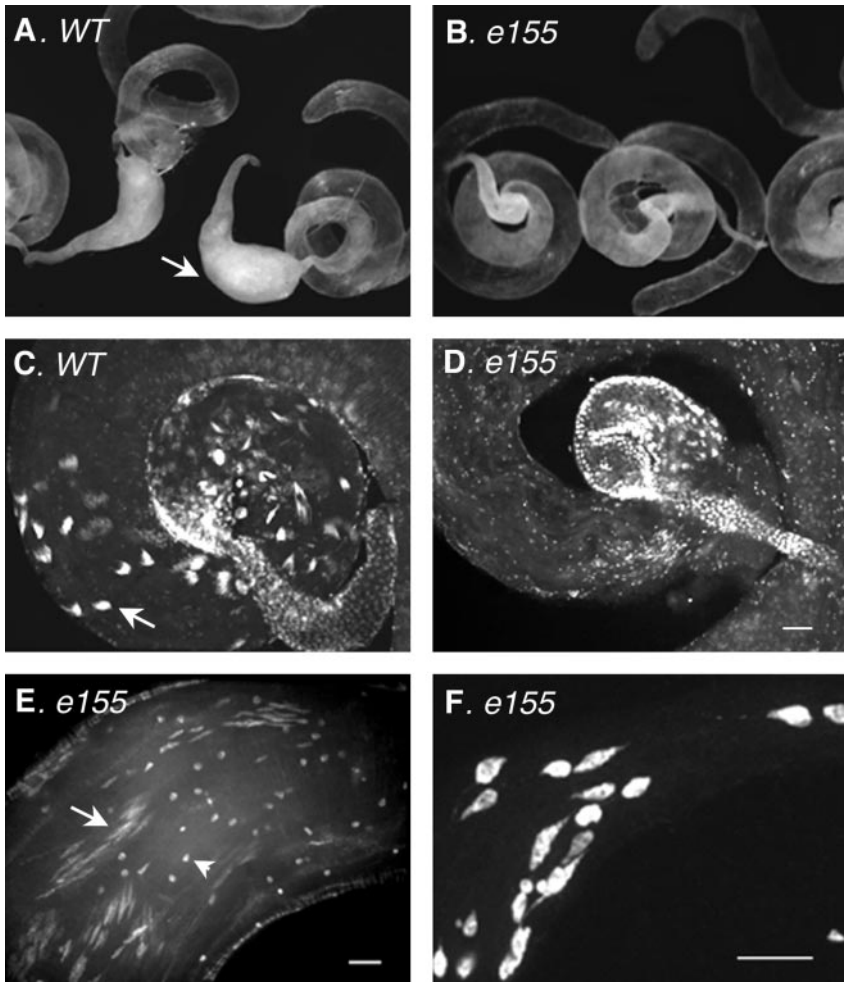

Figure 4. Morphology of mutant testis and spermatid nuclei. Testis morphology was examined using a phase-contrast microscope. Testes were dissected from wild-type (A) and *e155/e155* adult males (B) held away from females for 6 d. The base of a testis is located in the center of the coil. Arrow points to seminal vesicle. (C–F) Confocal sections of testes from 1- to 2-d-old adult males stained with fluorescent Oligreen dye to visualize nuclei. (C) Elongated and bundled spermatid nuclei in each cyst are visible near the base of wild-type testis (arrow). (D) In the *e155* mutant, nuclei are not properly bundled and seem scattered throughout the length of the testis. (E) Nuclei of *e155* mutant spermatids are scattered along sperm tails of several cysts seen in high magnification. Some nuclei have undergone proper elongation (arrow), whereas others have not (arrowhead). Region shown is near base of testis. (F) Scattered nuclei in a single cyst from *e155* mutant testis. Nuclei have not successfully elongated and are randomly oriented. Bar (C–F), 10 μm.

rhodopsin from the endoplasmic reticulum to the rhabdomere is important for the development and function of invertebrate photoreceptors (Kumar and Ready, 1995). However, we found no evidence that the 14-kDa LC is important for polarized transport in rhabdomere development. The *e155/e155* mutant flies do not exhibit a rough-eye phenotype as observed by scanning electron microscopy, and no obvious retinal degeneration was observed by imaging rhabdomeres by using an optic neutralization technique (our unpublished data). In addition, we assayed whether the null mutant exhibits a defective light response by recording the ERG, which measures the light-evoked electrical response of the retina. The ERG recorded from *e155/e155* flies was normal in appearance and in amplitude (see MATERIALS AND METHODS; supplemental Figure 1).

Spermatogenesis of Dlc90F *Mutant Males*

Spermatogenesis in *Drosophila* is well characterized (reviewed in Fuller, 1993). It begins with the stem cell divisions that give rise to founder spermatogonial cells. At the apical end of the testis, primary spermatogonia go through four synchronous mitotic divisions to give rise to a cyst of 16 spermatocytes. Subsequently, the 16 spermatocytes undergo two meiotic divisions to generate 64 spermatids. As a consequence of incomplete cytokinesis during both mitotic and meiotic cell divisions, the 64 postmeiotic spermatids are interconnected by cytoplasmic bridges in a common cyst. Next, the flagellar axonemes are assembled from basal bodies embedded in each spermatid nucleus. As the axonemes elongate, nuclear shape is streamlined and the spermatid nuclei are driven toward the basal end of the testis. After elongation, the syncytial spermatids are separated into individual sperm by an individualization complex (IC), a cone-shaped complex of cytoskeletal and membrane proteins that translocates the length of the cyst from the nuclei to the ends of the tails, eliminating excess cytoplasm and investing each sperm in its own membrane. Finally, the sperm bundles coil and motile spermatozoa are moved into the seminal vesicles.

Gross examination showed no morphological abnormality in the testes of the *Dlc90F* mutant males. However, the seminal vesicles of *Dlc90F* mutants did not swell after they were held away from females for several days. Under these conditions, we find no motile sperm in the mutant testes, whereas wild-type seminal vesicles accumulate motile sperm and look swollen (Figure 4). In *e155/e155* mutant testes, cysts at the 16-spermatocyte stage seem to be normal. Both mitotic and meiotic figures are readily seen using phase-contrast microscopy, suggesting that any defect is postmeiotic. Early "onion stage" spermatids present a typical, geometrically regular pattern within the cyst, as the 64 nuclei are each paired with a similarly sized spherical mitochondrial derivative. Flagella elongate, although sperm tails are bundled less tightly than those of wild type, and the coiling of tails in the mutant is compromised and less com-

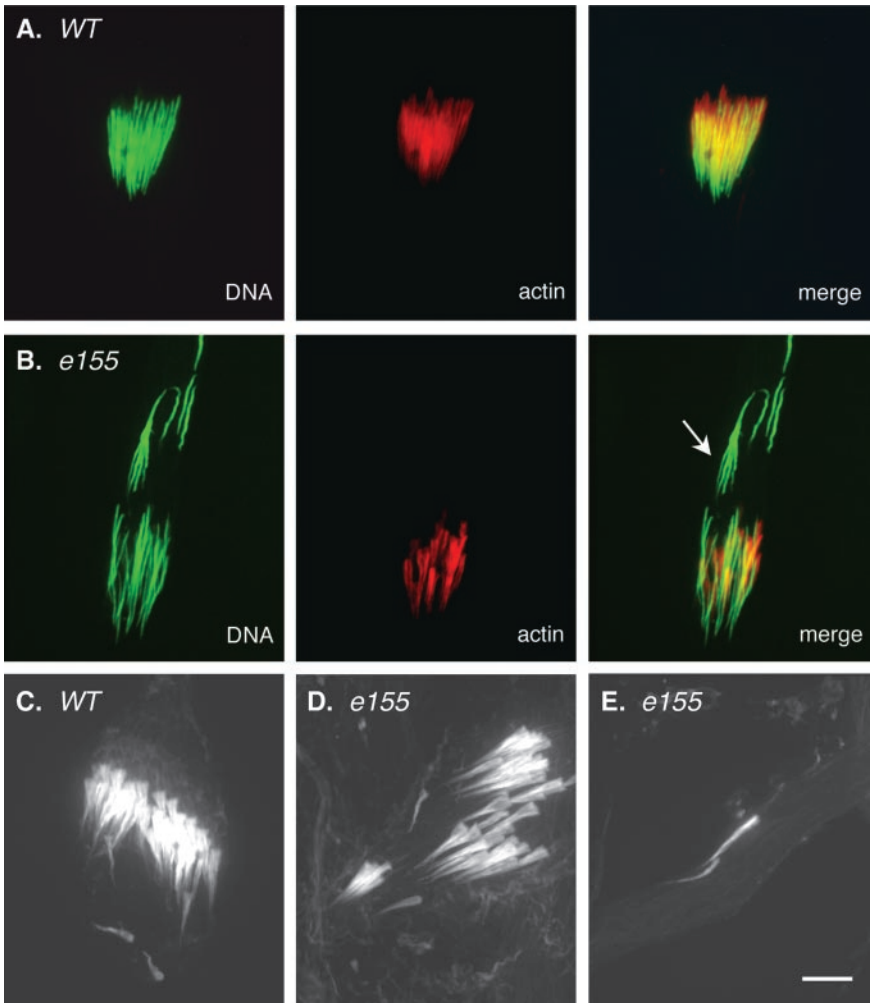

Figure 5. Individualization process. Testes were double stained with the DNA dye Oligreen to visualize spermatid nuclei (green) and rhodamine-conjugated phalloidin to visualize F-actin (red) in IC. Projected confocal images are shown. The base of testis is toward bottom; direction of IC movement is upwards. (A) In wild-type testes, fully elongated spermatid nuclei are tightly bundled and positioned in the end of each cyst. Actin cones, here associated with the nuclei, will travel toward the apical end of the testis. (B) Some nuclei of a cyst from *e155/e155* testis are positioned in the end of a cyst, are fully elongated, and associate with actin cones. Note mispositioned nuclei are not associated with actin cones (arrow). (C–E) Black- and-white images show actin staining only. (C) As the IC moves away from nuclei of a wild-type cyst, the actin cones assume amore triangular shape. The cones are tightly aligned and move synchronously. (D) Actin cones in the mutant line have formed a normal shape as they move away from nuclei, but are not properly aligned. (E) Two actin cones, presumably initiated from two fully elongated spermatid nuclei, have traversed asynchronously along sperm tails in the null mutant. Bar, 5 μm.

pact. Examination of mutant testes using electron microscopy showed that axonemal structure is not grossly affected by loss of the 14-kDa LC (our unpublished data).

To determine the defect in spermiogenesis, mutant testes were first stained with a fluorescent DNA dye to visualize nuclear shape and positioning. In wild type, the 64 spermatid nuclei in a cyst elongate together in a synchronized manner, aligned in parallel and positioned toward the basal end of each cyst. The elongated nuclear bundles are located within the basal third of a wild-type testis (Figure 4C). In testes from the 14-kDa null mutant, spermatid nuclei are not aligned or bundled at the end of the cyst (Figure 4D). Instead, spermatid nuclei within each cyst are scattered and positioned in varied orientations along the entire length of the cyst. In addition, mispositioned nuclei frequently fail to elongate or only partially elongate (Figures 4D, 5, and 7). Mutant nuclei that do maintain a normal position at the basal end of the cyst seem to elongate normally.

The aberrant organization of sperm tails seen by phase-contrast microscopy could result from defects in sperm individualization (Fabrizio *et al*., 1998). To examine this possibility more closely, we double-stained mutant testes to visualize DNA and F-actin filaments. The IC comprises 64 cones of actin that form around the spermatid nuclei after elongation and DNA condensation (Fabrizio *et al*., 1998; Rogat and Miller, 2002; Noguchi and Miller, 2003). Despite the mispositioning of most spermatid nuclei within the mutant cyst, the individualization process in the mutant seemed remarkably normal. Cones of actin were assembled and translocated along the axonemes (Figure 5). Typical groups of actin cones were observed moving away from the nuclear heads. In some cases, individual cones were observed in the middle of a sperm tail bundle, but nonetheless seemed to have assembled normally (Figure 5). These results argue that the individualization machinery in mutant testes is functional and that the observed defects in the individualization of spermatids are secondary, possibly due to the aberrant positioning of nuclei throughout the cyst of elongating spermatids.

The 14-kDa LC Acts to Mediate Cytoplasmic Dynein Localization at Nuclear Membranes of Early Spermatids

We examined the distribution of cytoplasmic dynein in the wild-type and 14-kDa LC null mutant. We visualized the cytoplasmic dynein motor by using a monoclonal antibody specific for the *Dhc64C* dynein heavy chain. Throughout spermatogenesis, a pool of cytoplasmic dynein seems to be homogeneously distributed. In wild-type early spermatids (i.e., onion stage), a striking concentration of cytoplasmic dynein in a hemispherical "cap" over one side of the nucleus is observed (Figure 6). No obvious enrichment of dynein in other stages of spermatogenesis was obtained under our experimental conditions. To verify the observed pattern of

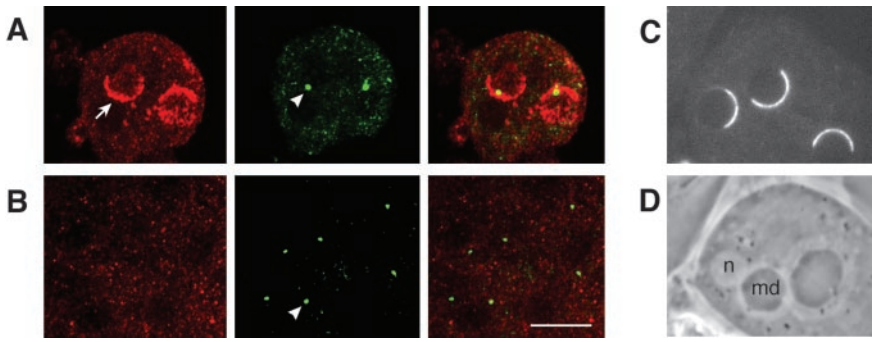

Figure 6. Cytoplasmic dynein localization in onion stage spermatids. Confocal images of fixed testes show dynein HC (red), and centrosomin (green). Pseudocolored channels are shown separately and merged. (A) In wild-type, dynein is enriched in a semicircular pattern (arrow) along the nuclear membrane adjacent to the basal body (arrowhead). (B) In the 14-kDa LC null, the distinct dynein localization is lost. (C) Live cells expressing a GFP-tagged subunit of dynactin (p50-GFP) confirm the concentrated semicircular localization of dynein motor at the nuclear membrane. Only the GFP signal is shown. (D) Phase-contrast image of wild-type spermatid illustrates relative positions and sizes of nucleus (n) and mitochondrial derivative (md). Bar, 5 μm.

dynein localization, we used a transgene encoding a GFP-tagged p50 dynamitin subunit of dynactin. The p50-GFP transgene is driven by the endogenous promoter and can fully rescue a lethal mutation in the p50 dynactin subunit (Wojcik *et al*., 2001). The p50-GFP gene product shows an identical pattern of localization to a hemispherical cap on early spermatid nuclei (Figure 6C). Previous studies have shown that in onion stage spermatids, a second layer of nuclear membrane comes to form a hemispherical cap on one side of the nucleus (Tates, 1971). In *Dlc90F* mutants, the hemispherical pattern of dynein localization is lost or greatly diminished, suggesting that the 14-kDa LC acts to mediate the association of cytoplasmic dynein with the nuclear membrane (Figure 6).

The nuclear cap enriched for cytoplasmic dynein and dynactin in wild-type spermatids lies juxtaposed to the newly formed basal body, as marked by an antibody against centrosomin (Figure 6). We reasoned that dynein localization at the nuclear membrane might help to maintain attachment of spermatid nuclei to the spermatid basal bodies. To explore this possibility, nuclei and basal bodies were visualized by staining for DNA and γ-tubulin, respectively, in elongating cysts. In wild-type, each of 64 nuclei is closely linked with a basal body throughout elongation and individualization (Figure 7A). In contrast, in *Dlc90F* mutant testes, few nuclei were seen to tightly associate with the basal body. As predicted, nuclei found in the middle of sperm tail bundles were not associated with a basal body (Figure 7, B and C). The few nuclei that maintained proper position at the basal end of the testis also seemed to maintain close linkage to the basal body.

DISCUSSION

Here, we demonstrate that the dynein 14-kDa light chain is not essential in *Drosophila*. Our data indicate that this *Drosophila* dynein subunit is only necessary for proper postmeiotic spermatid development and male fertility. This restricted phenotype distinguishes the 14-kDa light chain from other dynein subunits and supports the hypothesis that cytoplasmic dynein subunits can mediate specific dynein functions.

Diversity of Dynein Function: Roles of Subunits

If the subunits of cytoplasmic dynein provide its functional diversity, then mutations in different subunits might be expected to generate different phenotypes. Yet to date, strong loss-of-function mutations in different cytoplasmic dynein subunits show extensive overlap in the resulting mutant phenotypes. Beyond the heavy chain motor subunit, the intermediate, light intermediate, and light chains seem to be important in multiple dynein functions, but exactly how individual subunits contribute to the diversification of dynein function is not clear.

To date, some of the strongest evidence that dynein subunits can be functionally specialized comes from the analysis of the light chains in mammalian cells. Studies of rhodopsin transport in mammals reveal unique functions for specific LC family members. The tctex-1–dependent transport of rhodopsin can be inhibited by the overexpression of rp3 light chain, which does not bind rhodopsin, but competes for binding to the IC (Tai *et al*., 1999, 2001). Thus, tctex-1 and rp3 are not functionally redundant light chain isoforms. The *Drosophila* visual system shares many structural and functional features with the vertebrate visual system. Similar to the vertebrate system, rhodopsin photopigments move through the endoplasmic reticulum and Golgi and then are transported to the apical surface of the photoreceptor cells for incorporation into the specialized membranes of the rhabdomere. *Drosophila* rhabdomeres are the functional equivalent of the vertebrate membrane discs in the photoreceptor outer segment. In *Drosophila*, rhodopsin accounts for ~65% of membrane proteins in rhabdomeres and mutations in the rhodopsin gene *ninaE* cause rhabdomere degeneration (Kurada and O'Tousa, 1995). As in vertebrates, *Drosophila* cytoplasmic dynein is implicated in rhabdomere assembly by its participation in apical vesicle transport during rhabdomere morphogenesis (Fan and Ready, 1997). However, the null *Dlc90F* mutant displays normal rhabdomere development, and we found no alteration in the electroretinogram recorded from the 14-kDa LC null mutant compared with the control sibling flies. Given the essential requirement for rhodopsin in phototransduction, we conclude that the transport of rhodopsin is not defective in the null mutant and so does not depend on the 14-kDa LC in *Drosophila*.

Functional Redundancy and Nonessential Regulatory Functions for the 14-kDa LC

We have considered the possibility that another functionally redundant protein compensates for the loss of *Dlc90F*. Is another related light chain encoded by the *Drosophila* genome? Our results and others have shown there is only a single *tctex-1* family member in *Drosophila* (Caggese *et al*., 2001). We used low-stringency Southern blots and extensive database searches to rule out the existence of a second related gene. Thus, any essential function of the 14-kDa LC protein in rhodopsin transport or any other process is not being masked by the presence of multiple related genes. However, we cannot exclude the possibility that an unre-

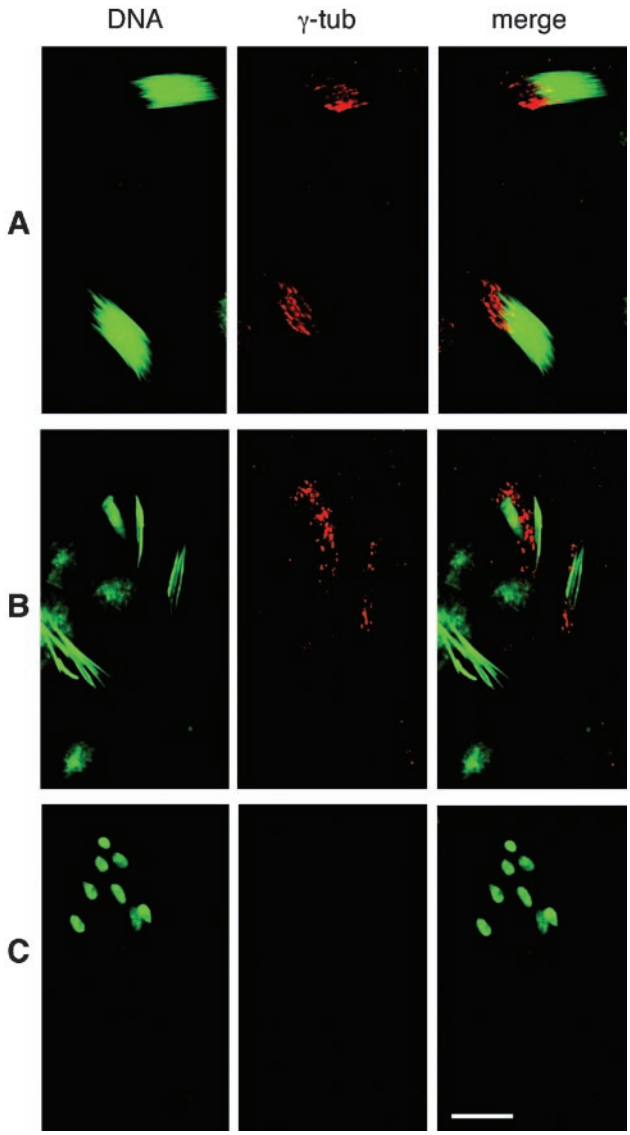

Figure 7. Detachment of spermatid nuclei from basal bodies. Confocal images were collected from testes stained to show DNA (green) and γ-tubulin (red). (A) In wild-type cysts, all 64 spermatid nuclei are elongated, tightly bundled, and attached to basal bodies, which are visualized here by γ-tubulin. (B) At the basal end of the mutant testis, few of the 64 nuclei have elongated properly. Elongated nuclei are less tightly bundled, with fewer nuclei in each bundle. Some are in the vicinity of the basal body, but few are actually attached. (C) Nuclei that are severely mispositioned and scattered in the middle of a mutant sperm tail bundle do not associate with basal bodies. Bar, 5 μm.

lated polypeptide can functionally compensate for the loss of *Dlc90F*.

Although the phenotype of the 14-kDa LC null is restricted to spermiogenesis, this does not reflect an absence of this subunit from dynein motors involved in other processes. *Dlc90F* gene expression is not restricted to testis and is abundant in ovaries and early embryos (Caggese *et al*., 2001; our unpublished data). We show that the 14-kDa LC cosediments on sucrose gradients with the 19S motor complex in microtubule affinity-purified cytoplasmic dynein. Because the function of cytoplasmic dynein is essential during early development, the viability of the null *Dlc90F* mutant demonstrates that the dynein motor complex can assemble and function in the absence of the 14-kDa light chain. On the other hand, the robust expression of this light chain and its assembly into the 19S complex suggest that an additional, nonessential dynein regulatory function is yet to be understood.

The *Drosophila* 14-kDa LC subunit may not always associate with the dynein motor complex. Our immunoblot analyses of fractionated whole ovary and embryo extracts reveal that the majority of the 14-kDa LC subunit does not cosediment with the 19S complex and is present in a "free" pool of light chain. Previously, Tai *et al*. (1998) reached a similar conclusion based on immunocytology and immunoprecipitation experiments in mammalian cells. The free pool of the 14-kDa LC may represent the dynamic assembly of the dynein complex. Alternatively, the 14-kDa light chain may function in other cellular process outside the dynein motor pathway and in doing so interact with and regulate other proteins. This possibility was previously demonstrated for the LC8 dynein light chain in its role as a component of both the myosin V and nitrous-oxide synthase complexes. Nonetheless, the limited phenotype of the 14-kDa LC null argues against this polypeptide acting in many places outside the dynein motor in *Drosophila*.

The Roles of the 14-kDa LC in Spermatid Differentiation

Our data provide new findings that show the 14-kDa LC is dispensable for most cytoplasmic dynein functions, but it is required for differentiation of spermatozoa in *Drosophila*. The *Dlc90F* null mutant is completely male sterile. A previous study of P element-induced mutations in this gene reported reduced fertility and sterility depending on the allele (Caggese *et al*., 2001). However, the mutations analyzed affected only the 5′ noncoding sequences and were inconclusive regarding the null phenotype. Moreover, no data on the cytological basis of the phenotype were presented. Our results establish the male sterile phenotype for a null 14-kDa LC mutant and shed light on the defects in spermatid development that underlie the observed sterility.

A striking defect observed in the *Dlc90F* null mutant testis was the mispositioning of spermatid nuclei during the elongation of flagellar axonemes. In a wild-type testis, all nuclei are maintained in a cluster as flagellar elongation takes place. By comparison, the mutant spermatid nuclei are not clustered but scattered along the entire length of the cyst. This defective nuclear position correlates with a disrupted linkage between the nucleus and the flagellar basal body. Immunolocalization of γ-tubulin, a component of the basal body, revealed that the basal body was no longer closely associated with the nucleus (Figure 7). During elongation, flagellar axonemes assemble from basal bodies embedded in each spermatid nucleus. As the axonemes elongate, the spermatid nuclei are moved toward the base of the testis. In the mutant, loss of the connection between the axoneme and nucleus may prevent maintenance of proper nuclear position within the elongating cyst.

How is the connection between the spermatid nucleus and flagellar basal body maintained? Our immunocytological observations reveal a novel nuclear cap of cytoplasmic dynein that lies juxtaposed to the associated flagellar basal body. Moreover, live imaging of a GFP-tagged dynactin component, p50-GFP, provides further evidence of the concentrated hemispherical cap of dynein. This distribution of dynein closely resembles the distribution of a second nuclear membrane that assembles and becomes limited to the nuclear side adjacent to the centriolar body (Tates, 1971). At this stage of spermatid differentiation, the centriole that will

insert into the nuclear envelope to become the basal body is surrounded by cytoplasmic microtubules. We speculate that the nuclear-associated dynein cap interacts with the cytoplasmic microtubules to facilitate the nuclear attachment and morphogenesis of the basal body. This hypothetical mechanism is supported by the observation that the nuclear cap of dynein localization and the nuclear attachment of basal bodies is greatly diminished or lost in the 14-kDa LC mutant background. Our experiments do not test whether the 14-kDa LC is directly involved in tethering dynein to the spermatid nucleus or, alternatively, affects expression of other dynein components during spermiogenesis. However, given the requirement for other dynein subunits throughout development, such an impact on expression would have to be unique to spermiogenesis. The association of cytoplasmic dynein and dynactin with the nuclear envelope of developing spermatids in mammalian cells has also been described and may be important in nuclear morphogenesis (Yoshida *et al*., 1994; Fouquet *et al*., 2000). Indeed, recent work has indicated that cytoplasmic dynein can associate with nuclei in a variety of cell types, and it has been implicated in nuclear migration, centriolar migration, and nuclear envelope breakdown (Xiang *et al*., 1994; Reinsch and Karsenti, 1997; Gonczy *et al*., 1999; Robinson *et al*., 1999; Salina *et al*., 2002). If the 14-kDa LC is involved in the targeting of cytoplasmic dynein in the *Drosophila* spermatid, then the viability and restricted phenotype of the *Dlc90F* mutant suggest that other mechanisms can regulate the nuclear localization of dynein outside the testis.

Axonemal versus Cytoplasmic Functions of the 14-kDa LC

Tctex-1 dynein light chain was previously shown to be a component of both cytoplasmic and axonemal dyneins. In *Chlamydomonas*, the 14-kDa subunit is a component of the I1 inner arm dynein involved in the regulation of flagellar waveform (King *et al*., 1996b). The lack of flagellar motility in the *Drosophila* 14-kDa LC mutant is consistent with the interpretation that this subunit is also a component of axonemal dyneins in *Drosophila*. The lack of flagellar motility is not likely due to loss of cytoplasmic dynein function, because mutant alleles of the cytoplasmic dynein heavy chain can be male sterile yet retain motile flagella (Gepner *et al*., 1996; Hays, unpublished data). In addition, in *Chlamydomonas*, mutations in the cytoplasmic dynein heavy chain or the associated LC8 light chain can inhibit assembly of the flagellar axoneme (Pazour *et al*., 1998; Porter *et al*., 1999). However, the *Drosophila* null 14-kDa LC mutant shows no such defect in flagellar assembly, suggesting that this light chain is not required for all cytoplasmic dynein functions in spermatid differentiation. Thus, although the loss of motility in flagellar axonemes could arise from the defect in cytoplasmic dynein function during basal body attachment, we do not favor this interpretation. Given the conservation of the cytoplasmic dynein light chains (tctex-1, LC8, and LC7/roadblock) across species, and given their shared role as axonemal dynein components in *Chlamydomonas*, it is likely that the light chains in *Drosophila* are also components of both cytoplasmic and axonemal dyneins.

ACKNOWLEDGMENTS

We thank the members of the Hays laboratory for helpful discussion and critical reading of the manuscript. We thank Pat Rosen for technical support and Polina Markovich for preparation of fly food. We acknowledge Matthew Pettit and Norbert Perrimon for sharing information on the insertion site of *l(3)0508*. This work was supported by a grant to T.S.H. from the National Institutes of Health (GM-044757).

REFERENCES

Bauch, A., Campbell, K.S., and Reth, M. (1998). Interaction of the CD5 cytoplasmic domain with the Ca2+/calmodulin-dependent kinase IIdelta. Eur. J. Immunol. *28*, 2167–2177.

Bowman, A.B., Patel-King, R.S., Benashski, S.E., McCaffery, J.M., Goldstein, L.S., and King, S.M. (1999). *Drosophila* roadblock and *Chlamydomonas* LC *7*, a conserved family of dynein-associated proteins involved in axonal transport, flagellar motility, and mitosis. J. Cell Biol. *146*, 165–180.

Boylan, K., Serr, M., and Hays, T.S. (2000). A molecular genetic analysis of the interaction between the cytoplasmic dynein intermediate chain and the glued (dynactin) complex. Mol. Biol. Cell *11*, 3791–3803.

Caggese, C., Moschetti, R., Ragone, G., Barsanti, P., and Caizzi, R. (2001). *dtctex-1*, the Drosophila melanogaster homolog of a putative murine t-complex distorter encoding a dynein light chain, is required for production of functional sperm. Mol. Genet. Genom. *265*, 436–444.

Campbell, K.S., Cooper, S., Dessing, M., Yates, S., and Buder, A. (1998). Interaction of p59fyn kinase with the dynein light chain, Tctex-1, and colocalization during cytokinesis. J. Immunol. *161*, 1728–1737.

Engels, W.R., Johnson-Schlitz, D.M., Eggleston, W.B., and Sved, J. (1990). High-frequency P element loss in *Drosophila* is homolog dependent. Cell *62*, 515–525.

Fabrizio, J.J., Hime, G., Lemmon, S.K., and Bazinet, C. (1998). Genetic dissection of sperm individualization in *Drosophila melanogaster*. Development *125*, 1833–1843.

Fan, S.S., and Ready, D.F. (1997). Glued participates in distinct microtubule-based activities in *Drosophila* eye development. Development *124*, 1497–1507.

Fouquet, J., Kann, M., Soues, S., and Melki, R. (2000). ARP1 in Golgi organisation and attachment of manchette microtubules to the nucleus during mammalian spermatogenesis. J. Cell Sci. *113*, 877–886.

Franceschini, N., and Kirschfeld, K. (1971). In vivo optical study of photoreceptor elements in the compound eye of *Drosophila*. Kybernetik *8*, 1–13.

Fuller, M.T. (1993). Spermatogenesis. In: The Development of *Drosophila melanogaster*, ed. M. Bate and A. M. Arias; Cold Spring Harbor, NY: Cold Spring Harbor Laboratory Press, 71–147.

Gepner, J., Li, M., Ludmann, S., Kortas, C., Boylan, K., Iyadurai, S.J., McGrail, M., and Hays, T.S. (1996). Cytoplasmic dynein function is essential in *Drosophila melanogaster*. Genetics *142*, 865–878.

Gill, S.R., Cleveland, D.W., and Schroer, T.A. (1994). Characterization of DLC-A and DLC-B, two families of cytoplasmic dynein light chain subunits. Mol. Biol. Cell *5*, 645–654.

Gonczy, P., Pichler, S., Kirkham, M., and Hyman, A.A. (1999). Cytoplasmic dynein is required for distinct aspects of MTOC positioning, including centrosome separation, in the one cell stage *Caenorhabditis elegans* embryo. J. Cell Biol. *147*, 135–150.

Harrison, A., Olds-Clarke, P., and King, S.M. (1998). Identification of the t complex-encoded cytoplasmic dynein light chain tctex1 in inner arm I1 supports the involvement of flagellar dyneins in meiotic drive. J. Cell Biol. *140*, 1137–1147.

Hays, T.S., Porter, M.E., McGrail, M., Grissom, P., Gosch, P., Fuller, M.T., and McIntosh, J.R. (1994). A cytoplasmic dynein motor in *Drosophila*: identification and localization during embryogenesis. J. Cell Sci. *107*, 1557–1569.

Kai, N., Mishina, M., and Yagi, T. (1997). Molecular cloning of Fyn-associated molecules in the mouse central nervous system. J. Neurosci. Res. *48*, 407–424.

Karki, S., and Holzbaur, E.L. (1999). Cytoplasmic dynein and dynactin in cell division and intracellular transport. Curr. Opin. Cell Biol. *11*, 45–53.

King, S. M., Barbarese, E., Dillman, J.F. 3rd, Patel-King, R.S., Carson, J.H., and Pfister, K.K. (1996a). Brain cytoplasmic and flagellar outer arm dyneins share a highly conserved Mr 8,000 light chain. J. Biol. Chem. *271*, 19358–19366.

King, S.M., Dillman, J.F. 3rd, Benashski, S.E. Lye, R.J., Patel-King, R.S., and Pfister, K.K. (1996b). The mouse t-complex-encoded protein Tctex-1 is a light chain of brain cytoplasmic dynein. J. Biol. Chem. *271*, 32281–32287.

Kumar, J.P., and Ready, D.F. (1995). Rhodopsin plays an essential structural role in *Drosophila* photoreceptor development. Development. *121*, 4359–4370.

Kurada, P., and O'Tousa, J.E. (1995). Retinal degeneration caused by dominant rhodopsin mutations in *Drosophila*. Neuron *14*, 571–579.

Lader, E., Ha, H.S., O'Neill, M., Artzt, K., and Bennett, D. (1989). tctex-1, a candidate gene family for a mouse t complex sterility locus. Cell *58*, 969–979.

Li, M.G., McGrail, M., Serr, M., and Hays, T.S. (1994). *Drosophila* cytoplasmic dynein, a microtubule motor that is asymmetrically localized in the oocyte. J. Cell Biol. *126*, 1475–1494.

Li, M.G., Serr, M., and Hays, T.S. (1998). Molecular and genetic characterization of gene encoding a 14kD dynein light chain in *Drosophila melanogaster*. Mol. Biol. Cell *9*, 153a.

Makokha, M., Hare, M., Li, M.G., Hays, T.S., and Barbar, E. (2002). Interactions of cytoplasmic dynein light chains Tctex-1 and LC8 with the intermediate chain IC74. Biochemistry *41*, 4302–4311.

McGrail, M., Gepner, J., Silvanovich, A., Ludmann, S., Serr, M., and Hays, T.S. (1995). Regulation of cytoplasmic dynein function in vivo by the *Drosophila* Glued complex. J. Cell Biol. *131*, 411–425.

McGrail, M., and Hays, T.S. (1997). The microtubule motor cytoplasmic dynein is required for spindle orientation during germline cell divisions and oocyte differentiation in *Drosophila*. Development *124*, 2409–2419.

Mok, Y.K., Lo, K.W., and Zhang, M. (2001). Structure of Tctex-1 and its interaction with cytoplasmic dynein intermediate chain. J. Biol. Chem. *276*, 14067–14074.

Mueller, S., Cao, X., Welker, R., and Wimmer, E. (2002). Interaction of the poliovirus receptor CD155 with the dynein light chain Tctex-1 and its implication for poliovirus pathogenesis. J. Biol. Chem. *277*, 7897–7904.

Nagano, F., Orita, S., Sasaki, T., Naito, A., Sakaguchi, G., Maeda, M., Watanabe, T., Kominami, E., Uchiyama, Y., and Takai, Y. (1998). Interaction of Doc2 with tctex-1, a light chain of cytoplasmic dynein. Implication in dynein-dependent vesicle transport. J. Biol. Chem. *273*, 30065–30068.

Noguchi, T., and Miller, K.G. (2003). A role for actin dynamics in individualization during spermatogenesis in *Drosophila melanogaster*. Development. *130*, 1805–1816.

Olds-Clarke, P. (1997). Models for male infertility: the t haplotypes. Rev. Reprod. *2*, 157–164.

Pazour, G.J., Wilkerson, C.G., and Witman, G.B. (1998). A dynein light chain is essential for the retrograde particle movement of intraflagellar transport (IFT). J. Cell Biol. *141*, 979–992.

Pfister, K.K., Salata, M.W., Dillman J.F. 3rd, Torre, E., and Lye, R.J. (1996a). Identification and developmental regulation of a neuron-specific subunit of cytoplasmic dynein. Mol. Biol. Cell *7*, 331–343.

Pfister, K.K., Salata, M.W., Dillman, J.F. 3rd, Vaughan, K.T., Vallee, R.B., Torre, E., and Lye, R.J. (1996b). Differential expression and phosphorylation of the 74-kDa intermediate chains of cytoplasmic dynein in cultured neurons and glia. J. Biol. Chem. *271*, 1687–1694.

Porter, M.E., Bower, R., Knott, J.A., Byrd, P., and Dentler, W. (1999). Cytoplasmic dynein heavy chain 1b is required for flagellar assembly in *Chlamydomonas*. Mol. Biol. Cell *10*, 693–712.

Rasmusson, K., Serr, M., Gepner, J., Gibbons, I., and Hays, T.S. (1994). A family of dynein genes in *Drosophila melanogaster*. Mol. Biol. Cell. *5*, 45–55.

Reinsch, S., and Karsenti, E. (1997). Movement of nuclei along microtubules in Xenopus egg extracts. Curr. Biol. *7*, 211–214.

Robinson, J.T., Wojcik, E.J., Sanders, M.A., McGrail, M., and Hays, T.S. (1999). Cytoplasmic dynein is required for the nuclear attachment and migration of centrosomes during mitosis in Drosophila. J. Cell Biol. *146*, 597–608.

Rogat, A.D., and Miller, K.G. (2002). A role for myosin VI in actin dynamics at sites of membrane remodeling during *Drosophila* spermatogenesis. J. Cell Sci. *115*, 4855–4865.

Salina, D., Bodoor, K., Eckley, D.M., Schroer, T.A., Rattner, J.B., and Burke, B. (2002). Cytoplasmic dynein as a facilitator of nuclear envelope breakdown. Cell. *108*, 97–107.

Silver, L.M. (1993). The peculiar journey of a selfish chromosome: mouse *t* haplotypes and meiotic drive. Trends Genet. *9*, 250–254.

Susalka, S.J., Hancock, W.O., and Pfister, K.K. (2000). Distinct cytoplasmic dynein complexes are transported by different mechanisms in axons. Biochim. Biophys. Acta *1496*, 76–88.

Tai, A.W., Chuang, J.Z., Bode, C., Wolfrum, U., and Sung, C.H. (1999). Rhodopsin's carboxy-terminal cytoplasmic tail acts as a membrane receptor for cytoplasmic dynein by binding to the dynein light chain Tctex-1. Cell *97*, 877–887.

Tai, A.W., Chuang, J.Z., and Sung, C.H. (1998). Localization of Tctex-1, a cytoplasmic dynein light chain, to the Golgi apparatus and evidence for dynein complex heterogeneity. J. Biol. Chem. *273*, 19639–19649.

Tai, A.W., Chuang, J.Z., and Sung, C.H. (2001). Cytoplasmic dynein regulation by subunit heterogeneity and its role in apical transport. J. Cell Biol. *153*, 1499–1509.

Tamkun, J.W., Deuring, R., Scott, M.P., Kissinger, M., Pattatucci, A.M., Kaufman, T.C., and Kennison, J.A. (1992). Brahma: a regulator of *Drosophila* homeotic genes structurally related to the yeast transcriptional activator SNF2/SWI2. Cell. *68*, 561–572.

Tates, A.D. (1971). Cytodifferentiation during spermatogenesis in Drosophila melanogaster: an electron microscope study. Ph.D. thesis, Rijksuniversiteit de Leiden, Leiden, The Netherlands.

Tynan, S.H., Purohit, A., Doxsey, S.J., and Vallee, R.B. (2000). Light intermediate chain 1 defines a functional subfraction of cytoplasmic dynein which binds to pericentrin. J. Biol. Chem. *275*, 32763–32768.

Wojcik, E., Basto, R., Serr, M., Scaerou, F., Karess, R., and Hays, T. (2001). Kinetochore dynein: its dynamics and role in the transport of the Rough deal checkpoint protein. Nat. Cell Biol. *3*, 1001–1007.

Xiang, X., Beckwith, S.M., and Morris, N.R. (1994). Cytoplasmic dynein is involved in nuclear migration in *Aspergillus nidulans*. Proc. Natl. Acad. Sci. USA *91*, 2100–2104.

Yano, H., Lee, F.S., Kong, H., Chuang, J., Arevalo, J., Perez, P., Sung, C., and Chao, M.V. (2001). Association of Trk neurotrophin receptors with components of the cytoplasmic dynein motor. J. Neurosci. *21*, RC125.

Yoshida, T., Ioshii, S.O., Imanaka-Yoshida, K., and Izutsu, K. (1994). Association of cytoplasmic dynein with manchette microtubules and spermatid nuclear envelope during spermiogenesis in rats. J. Cell Sci. *107*, 625–633.